

# Performance of a TCSC for Congestion Relief

Christian Schaffner, *Student Member IEEE*, Göran Andersson, *Fellow IEEE*

**Abstract**—This paper presents a method to determine the performance of relieving congestions using a Thyristor Controlled Series Capacitor (TCSC) in a transmission network by comparing locational marginal prices (LMP). The method allows to study different parameter variations – e.g. varying demand or size of the TCSC. A full AC Optimal Power Flow including transmission limits is used to model the underlying network. A case study shows the results of applying this method to a 10-bus network. The study is especially geared towards the economical evaluation of such an installation. However, the actual valuation is not part of this publication.

**Keywords**—liberalized electricity market, investment opportunities, FACTS, OPF, locational marginal prices (LMP).

## I. INTRODUCTION

IN recent years, need for economical efficiency and higher electricity consumption lead to an electric power transmission network with increased utilization. Even in highly meshed networks like in Europe this adds to the risk of local congestions in certain transmission lines or in links consisting of several lines. These congestions in turn can produce significant price differences between the areas around these congestions. Eliminating congestions by means of installing new transmission lines is normally difficult, if not impossible. It can take decades from evaluating a new line to the time it is installed. Political and environmental regulations further add to the difficulties improving the physical network.

### A. Today's Power Market

Currently, Italy pays significantly higher prices for electric energy than the rest of Europe: the prices per kWh is often twice as high in Italy than it is in France [1]. There are two main causes. *First*, the generation pattern is different in the two countries: France has mainly cheap production units based on nuclear or hydro power whereas the production mix in Italy is shifted significantly towards conventional thermal (oil and gas fired) units. The differences in the production mix do not necessarily cause price differences between the regions, although expensive production units may increase the overall prices if demand is high enough. The *second* – more significant – reason for the price difference is the limited transfer capacity between Italy and the rest of Europe. The link between Switzerland and Italy is at most times (during the day and during the year) loaded close to its capacity limits defined by network operators. It is the congestion that ultimately causes the price of electricity to be higher in Italy compared with neighboring European countries.

Ch. Schaffner and G. Andersson are with the EEH–Power Systems Group, Swiss Federal Institute of Technology (ETH), Zurich, Switzerland. (e-mail: schaffner@eeh.ee.ethz.ch, andersson@eeh.ee.ethz.ch)

Today, electric distribution systems are normally designed based on a (n-1)-security criterion. This means that the system must have enough security margins to operate even if one of the elements, e.g. a transmission line, fails. With congested inter-regional links this normally leads to the maximum allowed transfer capacity being considerably below the maximum power flow physically possible.

Controllable devices such as phase-shifting transformers or Flexible AC Transmission Systems (FACTS) allow the increase of the overall utilization of an electrical power network by controlling the power flow. Thus it is possible to relieve network congestions by increasing the Total Transfer Capacity (TTC) over a congested link.

In [2] the authors propose using a TCSC to relieve line overloads during contingencies, which increases the reliability of the whole system. They demonstrate the feasibility with different configurations on a 14-bus network. In addition, they clarify that not only network configuration and parameters influence functionality of the controllable devices but also influence load and generation patterns. Therefore accurate load and generation forecasts are an important part in the decision to invest in FACTS devices.

Another example is demonstrated in [3]: By installing a TCSC or an UPFC at one end of a parallel path the security of the system can be increased considerably, especially the loss of load probability.

The following sections present a methodology to model a congested network together with a TCSC to calculate locational marginal prices (LMP) at each node of the network.

## II. THE MODEL

The model we are using is based on the theory of the spot markets that has been developed by Fred C. Schweppe [4]. We are optimizing for *society welfare* thus assuming a perfectly competitive market where all participants behave rationally, have full and free access to market information and producers bid their marginal cost curves [5]. It is assumed that the consumers behave rationally, in that they do not purchase any good that has a higher price on the market than the benefit they would derive from it.

### A. TCSC Model

The TCSC is modeled as a series capacitor  $C$  in parallel with a thyristor controlled inductor  $L$  as shown in Fig. 1. Details about the modeling of FACTS devices can be found e.g. in [6].

For the optimization the TCSC is mathematically defined by its relation between the firing delay angle and the resulting series reactance  $X_{mn}^{TCSC}$  as shown in Fig. 2.

The susceptance  $B^{TCSC} (= X_{mn}^{TCSC^{-1}})$  is calculated as:

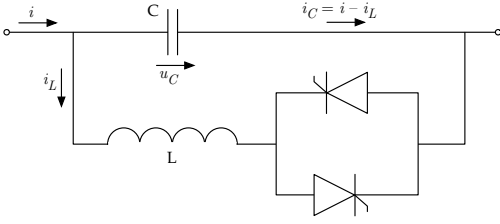


Fig. 1. TCSC model

$$B^{TCSC}(\alpha) = B_L \frac{\pi - 2\alpha - \sin 2\alpha}{\pi} + B_C \quad (1)$$

where  $B_L$  is the susceptance of the inductor  $L$  and  $B_C$  the susceptance of the capacitor  $C$  of the TCSC as shown in Fig. 1.  $B_L$  and  $B_C$  are defined as in Eq. (2). This presents the model for the fundamental system frequency equivalent.

$$B_L = \frac{1}{\omega L}, \quad B_C = -\omega C \quad (2)$$

$B_L$  has a positive and  $B_C$  a negative value. The resulting reactance  $X_{mn}^{TCSC}$  is shown for a thyristor firing delay angle between  $0^\circ$  and  $90^\circ$  in Fig. 2 as the solid line for the inductive ( $X_{mn}^{TCSC} > 0$ ) and the capacitive ( $X_{mn}^{TCSC} < 0$ ) region.

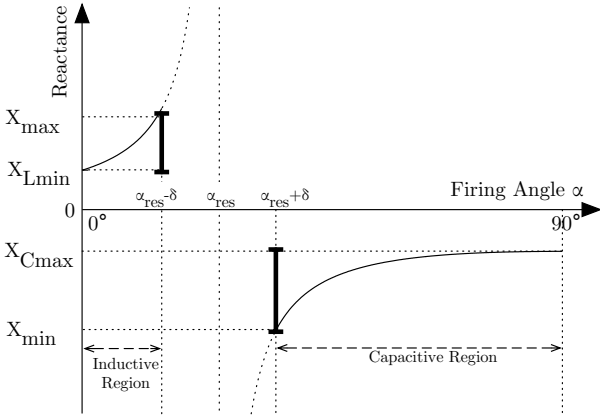


Fig. 2. Operating range of a TCSC (solid lines) and allowed regions for the reactance (bold lines)

The firing delay angle  $\alpha$  can be controlled between  $0^\circ$  and  $90^\circ$ . This results in a minimum reactance in the inductive region  $X_{Lmin}$  and a maximum reactance in the capacitive region  $X_{Cmax}$  defined as:

$$X_{Lmin} = \frac{1}{1/X_L + 1/X_C} = \frac{1}{B_L + B_C} \quad (3a)$$

$$X_{Cmax} = X_C = 1/B_C \quad (3b)$$

These values can be found by setting  $\alpha$  in Eq. (1) to  $0^\circ$  and  $90^\circ$ , respectively.

The TCSC has a resonance angle  $\alpha_{res}$  where the resulting inductive reactance is in resonance with the capacitive

reactance. A security margin  $\delta$  must be kept around the resonance angle  $\alpha_{res}$ :

$$\alpha < \alpha_{res} - \delta \quad \text{and} \quad \alpha > \alpha_{res} + \delta \quad (4)$$

In Fig. 2 the resonant angle  $\alpha_{res}$  is indicated as a dotted vertical line and the reactance in the inhibited operational region as dotted part of the curve.

The outer limits  $X_{min}$  and  $X_{max}$  have to be calculated using the resonance firing delay angle  $\alpha_{res}$  and the security margin  $\delta$ . These constraints are included in the optimization problem as linear inequality constraints.

### B. Optimization Method

An optimal power flow (OPF) algorithm is then used to optimize the so-called social welfare, subject to transmission constraints, generation limits, and TCSC limits. The mathematical setup is of the form:

$$\begin{aligned} & \text{minimize} && f(x) && x \in \mathbf{R}^n \\ & \text{subject to} && Ax - b = 0 \\ & && Cx - d \leq 0 \\ & && g_i(x) = 0 \\ & && h_j(x) \leq 0. \end{aligned} \quad (5)$$

where  $f(x)$  is the *objective function*,  $Ax - b = 0$  the linear equality constraints,  $Cx - d \leq 0$  the linear inequality constraints,  $g_i(x) = 0$  the non-linear equality constraints, and  $h_j(x) \leq 0$  the non-linear inequality constraints.

As the objective function the social welfare is used, as it is explained above. It is defined as:

$$SW = \underbrace{\sum_i B_i(P_{L_i}) - \lambda \cdot P_\lambda}_{CS} + \underbrace{\lambda \cdot P_\lambda - \sum_j C_j(P_{G_j})}_{PS} \quad (6)$$

where:

- $SW$  is the social welfare,
- $B_i$  the amount the consumer  $i$  is willing to pay for the power  $P_{L_i}$ ,
- $P_{L_i}$  the power consumed by load  $i$ ,
- $C_j$  the generator  $j$ 's cost to produce the power  $P_{G_j}$ ,
- $P_{G_j}$  the quantity of power produced by generator  $j$ ,
- $\lambda$  the price at the intersection of the consumers' and producers' aggregated marginal cost curves.
- $P_\lambda$  the power at the intersection of the aggregated marginal cost curves.

The term  $CS$  represents the consumer surplus and the term  $PS$  the producers' surplus (their profit).

Typical optimization algorithms minimize the objective function. Thus, the objective function to be minimized is:

$$f(P_{L_i}, P_{G_j}) = \sum_i B_i(P_{L_i}) - \sum_j C_j(P_{G_j}) \quad (7)$$

The cost curves of the generators are defined as quadratic functions (the index  $j$  is omitted in the following equations to increase legibility):

$$C(P_G) = a_0 + a_1 \cdot P_G + a_2 \cdot P_G^2 \quad (8)$$

These functions have to be monotonously increasing and convex to ensure a global maximum. Fig. 3 shows the quadratic cost curve (a) and the resulting marginal cost curve for a typical supplier (b). It is assumed that the suppliers bid continuous marginal cost curves.

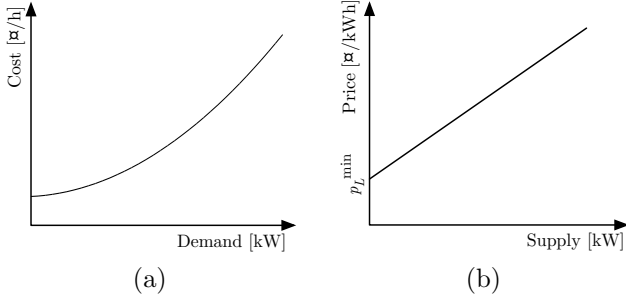


Fig. 3. Cost function for generators: Quadratic cost curve (a), corresponding marginal cost curve (b)

Concerning elastic demand, the specification of such a quadratic function is not appropriate, since the data needed for the determination of the coefficients is normally not known. Therefore, the maximum power consumption  $P_L^{\max}$  and the marginal price per kWh the consumer would pay for this quantity  $p_L^{\min}$  are defined. Accordingly the minimum power consumption  $P_L^{\min}$  and the marginal price per kWh  $p_L^{\max}$  are defined. The quadratic benefit function of a consumer then becomes (omitting the index  $j$  for legibility):

$$B(P_L) = b_1 \cdot P_L + b_2 \cdot P_L^2 \quad (9)$$

where

$$b_1 = P_L^{\max} \cdot m + p_L^{\min} \quad (10a)$$

$$b_2 = -m/2 \quad (10b)$$

$$m = \frac{p_L^{\max} - p_L^{\min}}{P_L^{\max} - P_L^{\min}} \quad (10c)$$

The parameter  $m$  is the slope of the line between the point  $(P_L^{\min}, p_L^{\max})$  and  $(P_L^{\max}, p_L^{\min})$  as illustrated in Fig. 4 (a). The quadratic benefit curve resulting from the integration of the marginal price curve is shown in Fig. 4 (b). It has to be monotonously increasing and concave to assure a global optimum for the optimization problem – ignoring the limits. This assumption can be justified by the expected behavior of consumers: The benefit function is increasing, since the consumer will pay more for a higher quantity consumed. The concavity results from the fact that consumers will try to first satisfy the power needs for processes, which produce the highest benefit. Therefore the change in benefit of buying more power diminishes for higher loads.

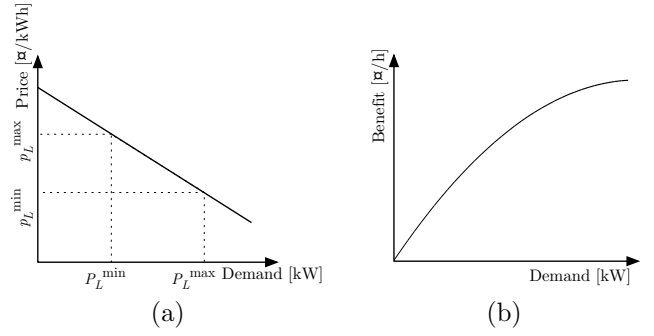


Fig. 4. Price and benefit functions for consumers: Maximum and minimum prices are set for minimum and maximum consumption (a), corresponding quadratic benefit function (b)

### C. Constraints

The linear inequality constraints are defined by the upper and lower production limits of the generators and the upper and lower consumption limits of the loads.

The non-linear equality constraints are defined by the active and reactive power balance in each node in the network. For node  $m$  the non-linear equation is defined as:

$$P_{G_m} - P_{L_m} - U_m \sum_{n_{con}} (U_n g_{mn} - U_n b_{mn} \sin(\delta_{mn}) - U_n g_{mn} \cos(\delta_{mn})) = 0 \quad (11)$$

for the active power and

$$Q_{G_m} - Q_{L_m} - U_m \sum_{n_{con}} (-U_m b_{mn} + U_n b_{mn} \cos(\delta_{mn}) - U_n g_{mn} \sin(\delta_{mn})) = 0 \quad (12)$$

for the reactive power, where

- $\sum_{n_{con}}$ : the sum over all nodes  $n$  connected to node  $m$ ,
- $P_{G_m}$ : the active power generated at node  $m$ ,
- $Q_{G_m}$ : the reactive power generated at node  $m$ ,
- $P_{L_m}$ : the active power consumed at node  $m$ ,
- $Q_{L_m}$ : the reactive power consumed at node  $m$
- $\delta_{mn}$ : the voltage angle difference between  $m$  and  $n$ ,
- $U_m$ : the voltage at node  $m$ ,
- $g_{mn}$ : the series conductance, and
- $b_{mn}$ : the series susceptance.

If a TCSC is built into the line between node  $m$  and node  $n$  the resulting reactance of the TCSC is entered in the series conductance and susceptance of the corresponding line by defining  $X_{mn} = X_{mn}^{line} + X_{mn}^{TCSC}$ . The reactance

between these two nodes is composed of a fixed part  $X_{mn}^{line}$  and a controllable part  $X_{mn}^{TCSC}$ , which is determined during optimization.

The non-linear inequality constraints ( $h_j(x) \leq 0$  in Eq. (5)) are given by the transmission capacity of the transmission lines and by the physical limits of the TCSC. For each line the limits are defined by

$$\left| U_m^2 g_{mn} - U_m U_n b_{mn} \sin(\delta_{mn}) - U_m U_n g_{mn} \cos(\delta_{mn}) \right| \leq P_{mn}^{max} \quad (13)$$

where

- $P_{mn}^{max}$ : the maximum power flow through the line  $mn$ .

The reactance  $X^{TCSC}$  is kept within the limits defined by Eq. (4) as shown in Fig. 2 by adding the corresponding non-linear inequality constraints.

The optimization algorithm now adjusts the dispatching of the generators, the flexible loads and the settings of the TCSC in order to maximize social welfare. The network is described as lists of generator, loads, lines and TCSCs with the associated nodes and respective parameters. The setup is very flexible allowing efficient simulation of parameter variations – e.g. the size of the TCSC, the load pattern, but also physical network changes.

For the actual optimization the Matlab™ “Optimization Toolbox” is used.

### III. CASE STUDY

In this section we present the application of the framework describe above to an example network where we show the influence of different parameter variations on the nodal electricity prices.

#### A. Modeled Network

The network used for the calculations is a ten-bus network with five generators and eight loads (see Fig. 5). In the top left region the cheapest generators (at node 3 and 5) are located whereas the region at the bottom has expensive production units at nodes 7 and 8. This will provoke energy flowing from the top left directly to node 7 and through nodes 1 and 2. Node 2 has only limited production capacity.

Due to the physical conditions of the network the link between nodes 1,2 and 9,10 is often congested. The cheap production units cannot export as much energy as they want into the bottom region, even though the direct connection line between node 6 and 7 still has transfer capacity available. The introduction of a TCSC device in this line will help to push more energy over this line and thus will decrease the prices in the bottom region.

The characteristics of the network can be described as follows:

- *Supply*: Large production units are installed in the top left area. Generator 2 is representing aggregated production of nuclear units. Generator 3 is an aggregation of

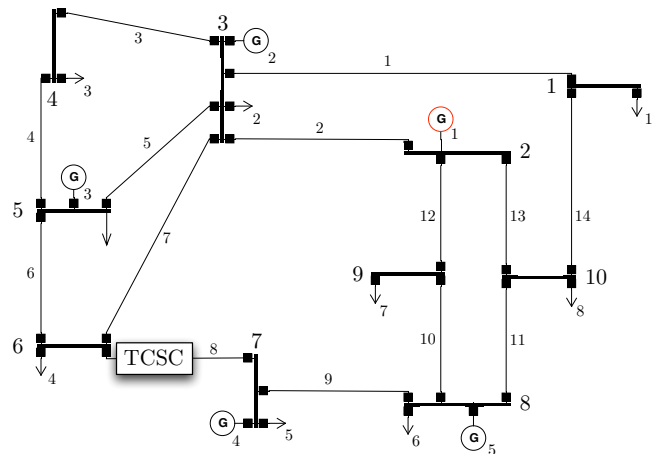


Fig. 5. 10 bus network used for simulations. A TCSC is installed in line 8 to force more power flow from the cheaper production area (generators 2 and 3) to the area with limited inexpensive capacity (generator 4).

conventional thermal units. Generator 1 and 4 represent hydro power installations, which have low production costs. The hydro production is rather small in comparison with other generators. Generator 5 in the lower right part of the network has high production costs (conventional thermal). The exact numbers can be found in table II. Only generator 1 is controlling the voltage to 1 p.u. The other generators do not produce reactive power.

- *Demand*: The large loads are number 2, 3, 5, 6, and 8 modeling two main load areas: One close to the production in the top left part of the network and one in the lower part close to the expensive thermal generator number 5. The demand elasticity is fairly small defined by the bandwidth of minimum and maximum demand as set in table III. The loads are assumed to only consume active power.
- *Transmission*: Due to the differences in production costs the power flow in the network is generally from the top left to-wards the bottom right. Therefore the total transfer capacity of lines 8, 12, 13, and 14 is significant for the simulation results. Line 8 has a fairly high TTC, but is – as the simulation results will show – normally not fully loaded.
- *Controllable Device*: A TCSC is installed in line 8 to control additional power transfers into the lower part of the network. The parameters of the TCSC modeled are shown in table I for three different scenarios: no TCSC (1), small TCSC (2), large TCSC (3). The TCSC is working in the capacitive region to compensate the line it is installed in, which is line 8 in this network. Table I shows the minimum resulting reactance and the maximum compensation degree the TCSC is capable of. The security margin  $\delta$  is set to  $10^\circ$ .

TABLE I

TCSC PARAMETERS FOR 3 DIFFERENT SIMULATION SCENARIOS.

	$X_C$ [p.u.]	$X_L$ [p.u.]	$X_{min}$ [p.u.]	Max. Comp. [%]
(1)				0%
(2)	-0.032	0.016	-0.9	59%
(3)	-0.048	0.024	-1.6	88%

### A.1 Network Parameters

The detailed electrical and economic parameters of the network components are shown below. For the generators, the economical and electrical parameters are defined in table II. For the loads, the parameters are set as shown in table III and for the lines as in table IV. The basis for the p.u. calculations is 1000 MVA.

TABLE II

GENERATOR PARAMETERS: GENERATOR 1 AND 4 ARE AGGREGATED HYDRO UNITS, GENERATOR 2 AGGREGATED NUCLEAR AND GENERATOR 3 AND 5 CONVENTIONAL THERMAL UNITS.

Nr.	$a_0$ [€]	$a_1$ [€/MW]	$a_2$ [€/MW <sup>2</sup> ]	$P_G$ [MW]
1	0	6.9	0.00067	1200
2	0	24.3	0.00040	8000
3	0	29.1	0.00006	3000
4	0	6.9	0.00026	800
5	0	50.0	0.00150	2000

TABLE III

LOAD PARAMETERS: THE PRICE SENSITIVITY IS SET TO BE LOW, RESULTING IN A SMALL BANDWIDTH BETWEEN  $P_L^{min}$  AND  $P_L^{max}$  COMPARED WITH THE PRICE DIFFERENCE BETWEEN  $p_L^{max}$  AND  $p_L^{min}$ .

Nr.	$P_L^{min}$ [MW]	$p_L^{max}$ [€/MW]	$P_L^{max}$ [MW]	$p_L^{min}$ [€/MW]
1	90	100	110	10
2	1300	100	1300	10
3	1300	100	1300	10
4	200	100	200	10
5	2400	100	2600	10
6	3400	100	3600	10
7	900	100	1100	10
8	1700	100	1900	10

### B. Results

This section presents the results applying the AC power flow model described above of the network in Fig. 5. For the evaluation of the TCSC varying demand scenarios are needed to model electricity prices throughout the day and over the valuation period. This is done by varying minimum and maximum load demand values ( $P_L^{min}$  and  $P_L^{max}$  in table III) between 60% and 100% linearly. The results of three different scenarios varying the TCSC size (as shown in table I) are presented below.

TABLE IV

TRANSMISSION LINE PARAMETERS: THE LINK BETWEEN THE HIGH PRICE AREA AND THE LOW PRICE AREA CONSISTS OF LINES 8, 12, 13, AND 14 RESULTING IN A THEORETICAL TOTAL TRANSFER CAPACITY OF 9.3 GW.

Nr.	$R$ [p.u.]	$X$ [p.u.]	$P_{mn}^{max}$ [MW]
1	0.04	0.10	3000
2	0.08	0.12	3500
3	0.01	0.10	1780
4	0.02	0.17	2150
5	0.02	0.17	2150
6	0.02	0.17	2800
7	0.02	0.17	3500
8	0.02	0.16	3500
9	0.02	0.25	2000
10	0.02	0.25	2260
11	0.01	0.07	3500
12	0.01	0.07	2260
13	0.01	0.14	1580
14	0.04	0.27	2000

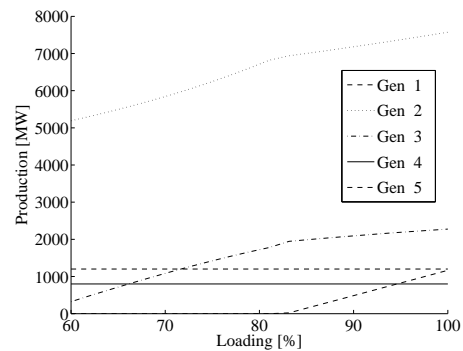


Fig. 6. Production of all generators in the network without TCSC: The expensive generator 5 only starts to produce if the prices are high enough (at a demand level of 84%).

### B.1 Results without TCSC

First, the OPF is calculated without any TCSC installed. Fig. 6 shows the output of the generators for demand levels between 60% and 100%. Generator 1 and 4, the hydro units, are always producing at the maximum capacity. Generator 1, which has the lowest production costs of the remaining generators, produces almost all the rest of the total power at a demand level of 60%. For increasing demand, generator 3 supplies a bigger part of the demand. Only at demand levels over 84%, the most expensive generator (number 5) starts to supply power. To explain this behavior of supply and demand, the resulting prices at different nodes have to be considered.

The prices at nodes 4, 6, 7, and 8 of the network are shown in Fig. 7. At low demand levels, the price differences between the top left part of the network (nodes 4 and 6) and the lower part of the network (nodes 7 and 8) result from

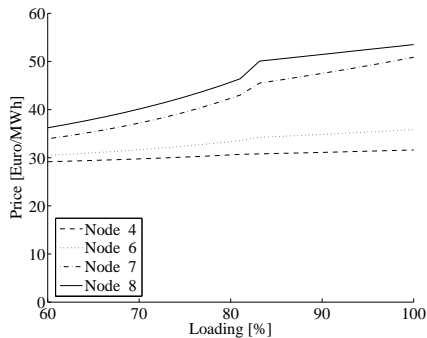


Fig. 7. Prices at nodes 4, 6, 7, and 8 without TCSC, if the loading is proportionally increased from 60% to a maximum of 100%.

the losses in the transmission network. Increasing demand, these differences grow larger. At a demand level of 82% and 84% the prices at the nodes in the lower area show a kink resulting from transmission constraints. Looking at the power flow through the transmission lines as shown in Fig. 8, line 13 reaches its TTC at a demand level of 82% limiting the power transfer into the high price area at the lower part of the network for higher demand levels. This results in the rise in nodal prices for nodes 7 and 8 between 82% and 84%.

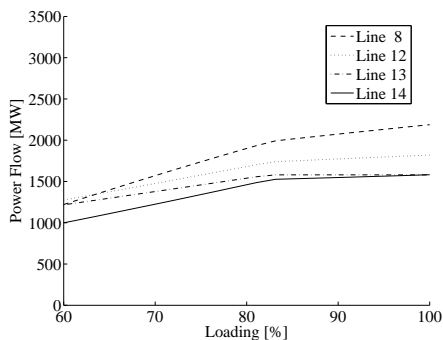


Fig. 8. Power flows through lines 8, 12, 13, and 14 linking the high price with low price area if no TCSC is installed. Line 13 reaches its transfer capacity at a demand level of 82%.

The higher prices resulting from demand levels above 84%, allow generator 5 to start producing energy. This production counteracts the rise in electricity prices for higher demands as can be seen in Fig. 7.

The next section shows the results of the same demand variations but with a TCSC installed in line 8. The TCSC should help transferring more energy over line 8 into the high price area.

### B.2 Results with small TCSC

The following figures show the results of the OPF simulation if a small TCSC (see table I row (2)) is installed. Fig. 9 shows the electricity prices. The kinks in the prices of the nodes in the high price area are less noticeable. Furthermore the effect is shifted to a demand level of around 90%.

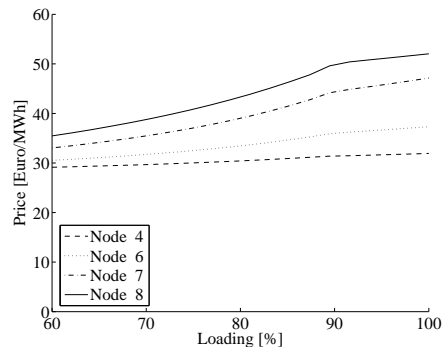


Fig. 9. Nodal prices at nodes 4, 6, 7, and 8 with a small TCSC compensating line 8, which reduces the price differences.

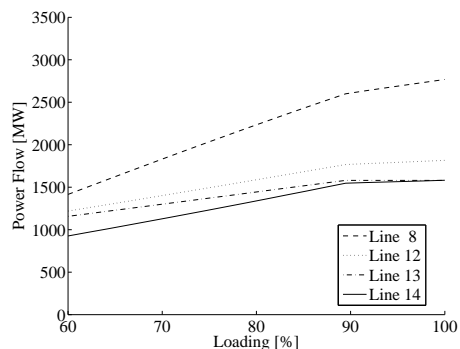


Fig. 10. Power flows if a small TCSC is installed. Compared with Fig. 8 line 8 carries significantly more power.

The TCSC is controlling the power flow as shown in Fig. 10. Comparing with the resulting flows without TCSC (see Fig. 8), the effect of the TCSC can be clearly shown: line 8 has a much higher power flow level, thus increasing the total imported energy into the high price area significantly. The demand level at which line 13 hits its transfer capacity is therefore shifted to the right to-wards a demand level of 90%.

On the supply side (see Fig. 11) the expensive generator 5 is now only producing energy above 90% demand level. The units with low production costs (generator 1 and 4) still produce at the maximum output level. But the cheap unit (generator 1) can produce more energy compared with the results without TCSC (see Fig. 6).

### B.3 Results with large TCSC

The following simulations show the results of the OPF calculations for a larger TCSC (see table I row (3)). Fig. 12 shows the electricity prices. The kink due to the power transfer limits of line 13 is shifted further to higher demand levels, now occurring at about 94%. This results in higher production levels from the cheap production of generator 1. The expensive generator 5 is only producing a small amount of power at the highest demand levels (see Fig. 13). It can also be noted that the price differ-

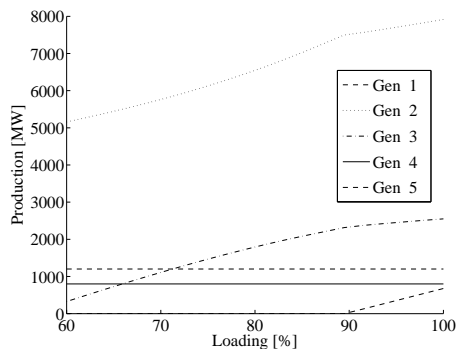


Fig. 11. Production of generators with a small TCSC compensating line 8.

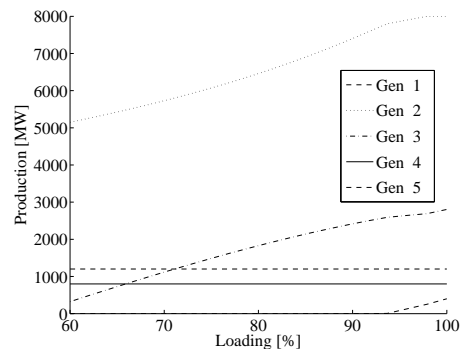


Fig. 13. Production of generators with a large TCSC compensating line 8.

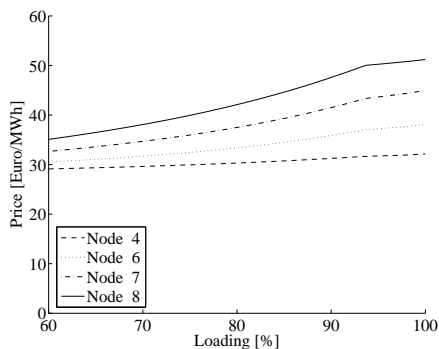


Fig. 12. Nodal prices at nodes 4, 6, 7, and 8 with large TCSC installed, reducing price differences even more compared with Fig. 9.

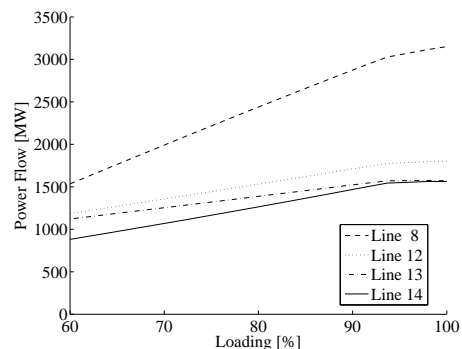


Fig. 14. Power flows if a large TCSC is installed. Line 8 carries even more power compared with the flows in Fig. 10.

ence for low demand levels between the nodes is significantly reduced compared with the results without TCSC (see Fig. 7).

Fig. 14 shows the power flows through the lines connecting the high and low price areas. Comparing with the smaller TCSC (see Fig. 10), line 8 carries even more power into the lower part of the network.

#### B.4 Discussion of Results

Comparing the nodal prices between the situation without any installed controllable device (Fig. 7) and the situation with a large TCSC (Fig. 12) it can be seen that the TCSC is not changing prices in low loading situations. The price of all nodes is almost equal between those two figures at 60% loading. However, as soon as there are lines becoming congested with higher loading values the price differences become significant looking at e.g. the prices at node 8.

### IV. CONCLUSIONS

This paper shows a possible approach to determine future electricity prices in a congested network as it is typically the case e.g. in Europe. A TCSC can be included in the model to study the influence of its operation on the nodal prices in the network. It is important to note that detailed analysis of the influence of a controllable device on

nodal prices is needed in order to understand its economical potential. Different loading situations can change the effectiveness of a controllable devices significantly.

The methodology to determine locational marginal prices presented in this is based on the assumption of a competitive market. This assumption is reasonable when looking at a time period of several decades. For a TCSC device to be an attractive investment opportunity the revenues for the company owning the TCSC should be paid from the congestion charges of the TSO.

### REFERENCES

- [1] "Statistical data on electricity in italy - synthesis 2003," 2003, <http://www.grtn.it/eng/statistiche/datistatistici03.asp>.
- [2] Y. Lu and A. Abur, "Static security enhancement via optimal utilization of thyristor-controlled series capacitors," *IEEE Transactions on Power Systems*, vol. 17, no. 2, pp. 324–329, 2002.
- [3] R. Billinton, M. Fotuhi-Firuzabad, S.O. Faried, and S. Abreshaid, "Impact of unified power flow controllers on power system reliability," *IEEE Transactions on Power Systems*, vol. 15, no. 1, pp. 410 – 415, 2000.
- [4] F.C. Schweppe, *Spot pricing of electricity*, Kluwer Academic Publishers, Boston [etc.], 1988, ISBN 0-89838-260-2.
- [5] J.D. Weber, T.J. Overbye, and P.W. Sauer, "Simulation of electricity markets with player bidding," in *Proceedings of the Bulk Power Systems Dynamics and Control IV*, Santorini, Greece, 1998, pp. 331–339.
- [6] N.G. Hingorani and L. Gyugyi, *Understanding FACTS: Concepts and Technology of AC Transmission Systems*, IEEE Press, New York, 2000, ISBN 0-471-20643-1.